

A feeling classification model in a blood draw situation using power spectrum density and a random forest algorithm

Rawinan Praditsangthong¹, Ekapong Nopawong²

¹College of Digital Innovation Technology (DIT), Rangsit University (RSU), Pathum Thani, Thailand

²Department of Computer Game and Esports, College of Digital Innovation Technology (DIT), Rangsit University (RSU), Pathum Thani, Thailand

Article Info

Article history:

Received Aug 16, 2024

Revised Jun 4, 2025

Accepted Jul 3, 2025

Keywords:

Anxiety

Blood draw

Classification

Feeling

Random forest

ABSTRACT

Feelings and expressions such as pain, anxiety, and excitement can occur while getting blood drawn. These are the physical symptoms that can occur in some patients. A medical provider cannot know pain or anxiety symptoms, which could cause harm to the patients throughout the procedure. However, electroencephalography (EEG) changes, such as Delta, Theta, Alpha, Beta, and Gamma, are essential to identify the patient's feelings. These can assist in decreasing danger during the procedures. Therefore, this research aims to investigate the patterns in the power spectrum density (PSD) form to classify two feeling states during blood drawing: normal and anxious feelings. This research focused on alpha, beta, and gamma of the PSD. Thus, a method was designed based on the changing values of alpha, beta, and gamma. Each PSD of three waves was derived at 56 minutes. The pattern from this dataset was applied to classify feeling expressions using a random forest (RF) algorithm. This algorithm was used to create a feeling classification model (FCM). The accuracy of the FCM in classifying feeling differences between normal and anxious feelings was 100%. Thus, this proves that the FCM is highly efficient.

This is an open access article under the [CC BY-SA](#) license.



Corresponding Author:

Ekapong Nopawong

Department of Computer Game and Esports, College of Digital Innovation Technology (DIT)

Rangsit University (RSU)

52/347 Mueng-Ake Village, Phahoyothin Road, Mueng, Pathum Thani, Thailand

Email: ekapong.n@rsu.ac.th

1. INTRODUCTION

Drawing blood is essential for medical treatment, such as for diabetes or high blood pressure. A patient often feels nervous or anxious while having blood drawn. Some patients can tell or express of pain or anxiety with a medical caretaker, while some patients do not express feelings, such as the voice or face. Moreover, medical caretakers do not notice an abnormality during the blood draw, which may cause danger.

One of the critical technologies is virtual reality (VR), which is applied to medical treatment, such as pain and anxiety management. By immersing users in an interactive virtual environment, VR effectively diverts attention from distressing medical procedures [1]-[2]. This distraction mechanism is especially useful in situations where patients experience heightened anxiety, such as during blood draws. Studies have shown that VR applications significantly reduce perceived pain and anxiety in pediatric and adult patients undergoing needle-related procedures [3]-[7]. The ability of VR to create engaging and immersive experiences makes it a promising tool for improving patient comfort during medical treatments [8]-[11]. In the context of this study, a VR-based intervention may serve as an effective means of mitigating anxiety by diverting the patient's attention from the discomfort associated with the blood draw procedure.

By analyzing electroencephalography (EEG) signals, the purpose of this study is to explore the impact of VR on anxiety levels and classify emotional states through machine learning (ML) techniques.

EEG refers to use to measure the brain's electrical activity. It is a powerful tool for studying brain function and has been used in various applications, including clinical diagnosis, research, and entertainment. EEG has five waves: Delta, Theta, Alpha, Beta, and Gamma. Each wave has a different frequency range of 13-30 Hz [12]. In case of excitement or anxiety, alpha waves will decrease in frequency, while beta waves will increase in frequency. EEG can assist in exploring a pattern of anxiety feeling. In addition, this helps in developing suitable applications for VR.

Currently, there is some equipment to help with simple EEG measurements, such as the brain-sensing headband. This headband has five or seven sensors, depending on the model, that measure EEG from different points on the head. Five sensors consist of the front forehead position in the middle (FP1), the right front forehead position (FP2), the front left position (AF3), the front proper position (AF4), and the left occipital position (O1). However, two additional sensors were added, the left (T7) and the right temples (T8), which can assist in more accurate measurement of brain waves [13]. Thus, EEG data from the seven sensors is used to calculate different brain waves, such as alpha, beta, and gamma waves [14]-[15].

Since EEG monitors brain activity through electrodes, it captures the electrical signals generated by neurons. These signals are amplified and digitized and can be analyzed using various techniques. Therefore, pattern investigation of feeling expression during procedures, blood drawing, or vaccination must be applied to EEG with ML algorithms. However, there are favorite ML algorithms in medical applications, such as neural networks (NNs), convolutional neural networks (CNNs), support vector machines (SVM), decision trees (DT), naive bayes, random forests (RFs), and k-nearest neighbors (KNNs) [16]. These algorithms are supervised learning techniques for classification and regression tasks. This technique needs a training dataset with correct features and labels. The resulting model must be tested for prediction accuracy on the testing dataset, knowing the model's efficiency.

All algorithms mentioned above, it is often used in medical image analysis for the prediction, diagnosis, and classification of disease. For instance, NN, including CNNs have been applied to tasks such as image recognition, lesion detection, and tissue classification [17]-[20]. SVM and DT have found applications in detecting heart disease, cancer, or major depressive disorder [21]-[25]. Furthermore, there is a comparison prediction or diagnosis accuracy of breast cancer disease from medical images with SVM, logistic regression, RF, and DT [26]. The results display that the logistic regression has better accuracy at 95%. However, EEG and ML techniques are also used in medical areas. There are uses of EEG in epilepsy with the RF method [27]. The dataset of the EEG signal contains more than 200 epilepsy signals, which are used to extract features. These features lead to the development of a model with an RF algorithm compared with SVM. The experiment displays that the RF algorithm has higher accuracy than the SVM. In addition, some research has applied EEG to asthma [28]. These EEG signals are used to define the severity level of asthma. Therefore, it is necessary to search for characteristics that indicate asthma symptoms at different levels of EEG signal severity. Similar to the research mentioned earlier, there are comparisons of the accuracy of disease severity prediction among several algorithms. The results show that the RF algorithm has the best accuracy.

As the reasons mentioned above, EEG is a non-invasive test that uses an EEG recorder to detect electrical waves in the brain. ML examines feature extraction to develop a classification model. The combination of EEG and ML is a tool too powerful for the medical area. Thus, this research is to investigate the pattern of the power spectrum density (PSD) from EEG to develop a feeling classification model (FCM) between normal and anxiety feelings using a RF algorithm in a blood draw situation. Section 2 is the methods of the research, which consists of the data collection, processing, and data analysis processing. Then, parameters, model creation, results, and discussion are described in section 3. Finally, the conclusion is elaborated in section 4.

2. METHOD

2.1. Data collection processing

The dataset was acquired from participants undergoing blood draw procedures as part of Rangsit University's annual health check-up on December 22, 2022. The data is collected using accidental random sampling. The researcher explained the steps involved in installing the equipment used to collect data before the target group agreed to participate as volunteers for the project. The research needs to use brain-sensing equipment like MUSE to measure EEG in Alpha, Beta, and Gamma in PSD form to classify two states of emotion during a blood draw: the normal state and the anxiety state. Thus, volunteers who agreed to the data collection must sign a consent form. Then, brain-sensing equipment (MUSE) is installed on the volunteer's head. It is attached to the forehead while measuring and will measure the PSD from the forehead and behind the ears. For each participant, four electrode points with AF7, AF8, TP9, and TP10 from the electrode are

collected in 4 minutes, as displayed in Figure 1. A total of 14 individuals volunteered to participate in the data gathering process.

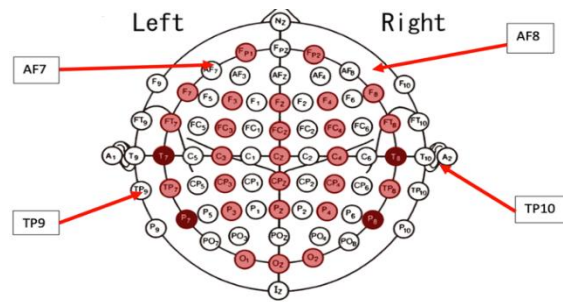


Figure 1. Electrode points

2.2. Data collection processing

The 56 minutes of the PSD consist of two datasets: one for training and the other for testing. There are 10 participants in the training set, while the testing set includes 4 participants. Moreover, all seconds of the PSD were calculated to define the differences between neutral feeling and anxiety feeling using the PSD from four electrode positions: AF7, AF8, TP9, and TP10.

After completing the data collection, 40 minutes of the PSD from the training dataset were retrieved, and the means of the PSD were determined in AF7, AF8, TP9, and TP10. In the training dataset, the 10 participants are 50.0% male and 50.0% female. The experimental results can be summarized as follows.

2.3. Mean and standard deviation of PSD of Alpha

This test is the PSD measurement of Alpha at the TP9, TP10, AF7, and AF8 points from M1 (0-1 min) to M4 (3-4 min) while drawing blood, as presented in Table 1. The results showed that the highest average of the TP9 point is minute one with mean = 0.71, SD = 0.15, while the highest average of the AF7 position is minute two with mean = 0.60, SD = 0.22. The AF8 point has the highest average at minute one with mean = 0.58, SD = 0.18. The last point is the TP10, which has the highest average at minute two, with mean = 0.63 and SD = 0.26.

Thus, the test shows the total average of all points from M1 (0-1 min) to M4 (3-4 min). The results presented that minute one and two have the highest average with mean = 0.61, SD = 0.20, and then the average decreases until minute 4. From Figure 2, the PSD of Alpha can show anxiety status.

Table 1. Means and standard deviations of TP9, TP10, AF7, and AF8 from Alpha (dB/Hz)

PSD of Alpha points	M1 (0-1 min)	M2 (1-2 min)	M3 (2-3 min)	M4 (3-4 min)
TP9	0.71 ± 0.15	0.64 ± 0.15	0.46 ± 0.99	0.18 ± 1.04
TP10	0.57 ± 0.26	0.63 ± 0.26	0.34 ± 0.79	0.43 ± 0.50
AF7	0.57 ± 0.16	0.60 ± 0.20	0.55 ± 0.19	0.56 ± 0.22
AF8	0.58 ± 0.18	0.57 ± 0.17	0.54 ± 0.14	0.57 ± 0.24
Total	0.61 ± 0.20	0.61 ± 0.20	0.47 ± 0.63	0.44 ± 0.60

2.4. Mean and standard deviation of PSD of Beta

This experiment is similar to the PSD of Alpha results, but the test changes the PSD from Alpha to Beta. Therefore, the highest average at M1 (0-1 min) has two points as the TP9 and AF8. The TP9 has a mean of 0.80 and SD = 0.21; the AF8 has a mean of 0.60 and SD = 0.25. The highest average at M2 (1-2 min) was the AF7, with mean = 0.85, SD = 0.39. The last point is the TP10; it has the highest average at M3 (2-3 min), with mean = 0.73, SD = 0.31. Table 2 shows the means and standard deviations of TP9, TP10, AF7, and AF8 of the PSD of Beta.

On the other hand, the total average of all points has no differences from M1 (0-1 min) to M4 (3-4 min), as displayed in Figure 3. Thus, this may not be enough to conclude that the PSD of Beta indicates a state of anxiety while drawing blood.

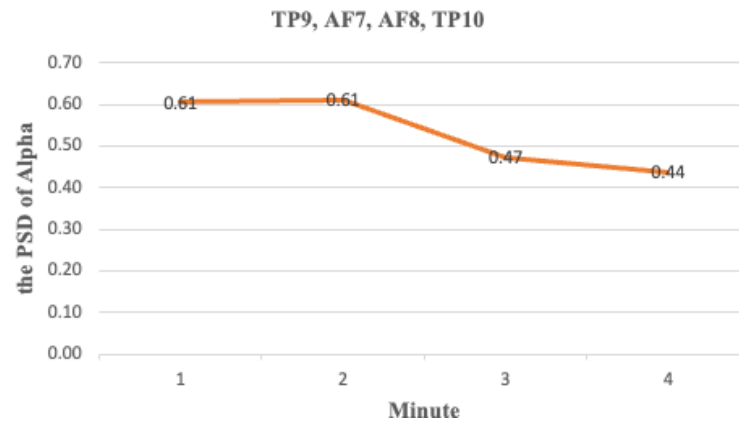


Figure 2. The level of the PSD of Alpha from every position

Table 2. Means and standard deviations of TP9, TP10, AF7, and AF8 from Beta (dB/Hz)

PSD of Beta Points	M1 (0-1 min)	M2 (1-2 min)	M3 (2-3 min)	M4 (3-4 min)
TP9	0.80 ± 0.21	0.63 ± 0.31	0.71 ± 0.33	0.48 ± 0.44
TP10	0.69 ± 0.31	0.61 ± 0.40	0.73 ± 0.31	0.39 ± 0.43
AF7	0.63 ± 0.24	0.85 ± 0.39	0.80 ± 0.35	0.52 ± 0.27
AF8	0.60 ± 0.25	0.56 ± 0.33	0.51 ± 0.33	0.47 ± 0.25
Total	0.68 ± 0.26	0.67 ± 0.37	0.69 ± 0.34	0.46 ± 0.35

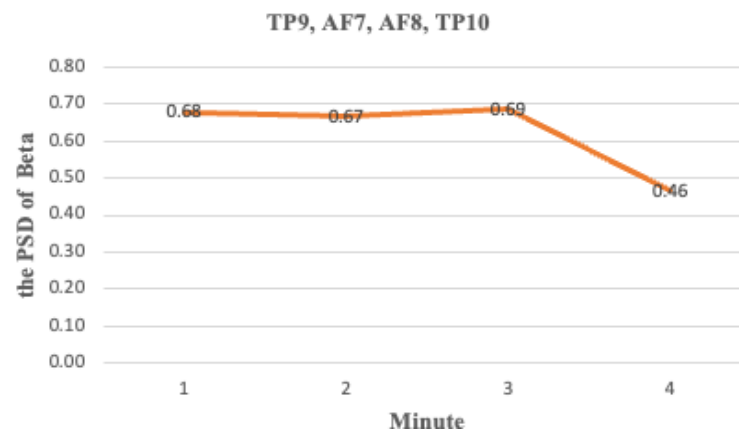


Figure 3. The level of the PSD of Beta from every position

2.5. Mean and standard deviation of PSD of Gamma

From the above results, the PSD of Beta cannot indicate the status of anxiety. Therefore, the PSD of Gamma is measured to explore the pattern of anxiety state while drawing blood. The test is similar to the PSD of Alpha and Beta. Table 3 displays the means and standard deviations of all points of the PSD of Gamma. All positions have the same highest average at minute three. The TP9 has a mean of 0.60, SD = 0.26, and AF7 has a mean of 0.74, SD = 0.50. Moreover, AF8 has a mean of 0.43, SD = 0.30, and TP10 has a mean of 0.61, SD = 0.36. From the PSD of Gamma result above, the PSD of Gamma can indicate the anxiety status since each position has a level of the PSD that moves up. Moreover, the total average of every point shows the PSD increase level from minute one to three. The highest average is minute three, with mean = 0.59, SD = 0.37, as presented in Figure 4.

Table 3. Means and standard deviations of TP9, TP10, AF7, and AF8 from Gamma (dB/Hz)

PSD of Gamma points	M1 (0-1 min)	M2 (1-2 min)	M3 (2-3 min)	M4 (3-4 min)
TP9	0.57 ± 0.27	0.56 ± 0.25	0.60 ± 0.26	0.46 ± 0.30
TP10	0.45 ± 0.34	0.59 ± 0.35	0.61 ± 0.36	0.50 ± 0.33
AF7	0.47 ± 0.25	0.73 ± 0.49	0.74 ± 0.50	0.51 ± 0.25
AF8	0.32 ± 0.25	0.35 ± 0.27	0.43 ± 0.30	0.32 ± 0.21
Total	0.45 ± 0.29	0.56 ± 0.37	0.59 ± 0.37	0.45 ± 0.28

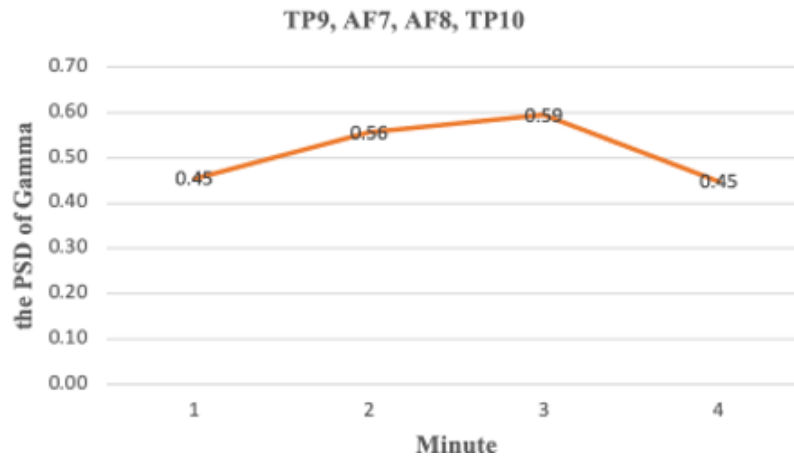


Figure 4. The level of the PSD of Gamma from every position

2.6. The difference in mean PSD of Alpha

This tests the PSD measurement of Alpha at TP9, TP10, AF7, and AF8 points from M1 (0-1 min) to M4 (3-4 min) while drawing blood. The results of TP9 position displayed that there are no significant differences between genders and the PSD, with a p -value = 0.903 > 0.05. The results of the AF7 position displayed that there are no significant differences between males and females in the PSD measurement and the AF8 position produced the same results, with a p -value = 0.999 > 0.5. Moreover, the last point is the TP10 showed that there are no significant differences between genders and the PSD, with a p -value = 0.936 > 0.05. Table 4 presents the mean PSD of Alpha with the standard deviations of both genders in the samples.

2.7. The difference in mean PSD of Beta

The experimental results are the test of the PSD of Beta at the TP9, TP10, AF7, and AF8 from M1 (0-1 min) to M4 (3-4 min) while drawing blood. The results displayed no significant difference between genders and three positions, such as the TP9, AF8, and TP10 positions, with exact p -value = 0.999 > 0.05. Moreover, there is no significant difference between males and females in PSD of Beta, with a p -value = 0.998 > 0.05. The mean PSD of Beta with the standard deviations is given in Table 5.

Table 4. Means TP9, TP10, AF7, AF8, and gender of Alpha with SD (dB/Hz)

Points	Gender	M1 (0-1 min)	M2 (1-2 min)	M3 (2-3 min)	M4 (3-4 min)
TP9	Male	0.71 ± 0.14	0.66 ± 0.15	0.77 ± 0.27	0.40 ± 0.40
	Female	0.72 ± 0.16	0.62 ± 0.16	0.05 ± 1.45	0.11 ± 1.55
TP10	Male	0.53 ± 0.22	0.63 ± 0.25	0.57 ± 0.36	0.50 ± 0.24
	Female	0.62 ± 0.32	0.64 ± 0.30	0.04 ± 0.12	0.33 ± 0.24
AF7	Male	0.54 ± 0.15	0.57 ± 0.20	0.49 ± 0.16	0.59 ± 0.26
	Female	0.61 ± 0.18	0.65 ± 0.24	0.64 ± 0.20	0.53 ± 0.19
AF8	Male	0.55 ± 0.19	0.56 ± 0.17	0.52 ± 0.14	0.53 ± 0.24
	Female	0.61 ± 0.19	0.58 ± 0.18	0.58 ± 0.14	0.64 ± 0.24

Table 5. Means TP9, TP10, AF7, AF8, and gender of Beta with SD (dB/Hz)

Points	Gender	M1 (0-1 min)	M2 (1-2 min)	M3 (2-3 min)	M4 (3-4 min)
TP9	Male	0.82 ± 0.20	0.74 ± 0.22	0.82 ± 0.27	0.53 ± 0.50
	Female	0.77 ± 0.18	0.50 ± 0.38	0.57 ± 0.38	0.41 ± 0.38
TP10	Male	0.67 ± 0.33	0.60 ± 0.42	0.77 ± 0.28	0.39 ± 0.47
	Female	0.71 ± 0.30	0.63 ± 0.40	0.68 ± 0.37	0.40 ± 0.40
AF7	Male	0.56 ± 0.20	0.80 ± 0.50	0.68 ± 0.40	0.54 ± 0.30
	Female	0.72 ± 0.28	0.92 ± 0.30	0.96 ± 0.23	0.49 ± 0.30
AF8	Male	0.54 ± 0.20	0.54 ± 0.40	0.48 ± 0.30	0.47 ± 0.30
	Female	0.68 ± 0.29	0.59 ± 0.31	0.55 ± 0.34	0.47 ± 0.20

2.8. The difference in Mean PSD of Gamma

Same as the previous experiment, this is the test of Gamma PSD at four points: the TP9, TP10, AF7, and AF8 from M1 (0-1 min) to M4 (3-4 min). At AF7 and AF8, there are no significant differences between genders and the Gamma, with exact p -value = 0.999 > 0.05. Moreover, there are no significant differences between males and females in the Gamma of the TP9 and TP10 positions, with a p -value = 0.998 > 0.05 and a p -value = 0.995 > 0.05, respectively. Table 6 shows the mean PSD of Gamma with the standard deviations.

Table 6. Means TP9, TP10, AF7, AF8, and gender of Gamma with SD (dB/Hz)

Points	Gender	M1 (0-1 min)	M2 (1-2 min)	M3 (2-3 min)	M4 (3-4 min)
TP9	Male	0.58 ± 0.34	0.65 ± 0.28	0.69 ± 0.31	0.52 ± 0.36
	Female	0.57 ± 0.17	0.43 ± 0.12	0.47 ± 0.11	0.38 ± 0.20
TP10	Male	0.41 ± 0.37	0.59 ± 0.43	0.72 ± 0.31	0.46 ± 0.37
	Female	0.50 ± 0.32	0.59 ± 0.23	0.47 ± 0.40	0.55 ± 0.28
AF7	Male	0.48 ± 0.27	0.70 ± 0.53	0.73 ± 0.52	0.47 ± 0.25
	Female	0.46 ± 0.25	0.76 ± 0.47	0.75 ± 0.52	0.55 ± 0.27
AF8	Male	0.34 ± 0.28	0.36 ± 0.32	0.42 ± 0.38	0.30 ± 0.23
	Female	0.30 ± 0.24	0.33 ± 0.23	0.43 ± 0.18	0.34 ± 0.19

3. RESULTS AND DISCUSSION

3.1. Parameter for model creation

From the above experimental results, three critical parameters can affect anxiety emotions: the PSD of Alpha, Beta, and Gamma. However, the PSD may relate to other parameters, such as gender and age. Thus, all parameters should be considered for creating a model to identify the feelings. This research's independent parameters are gender, age, and the PSD of Alpha, Beta, and Gamma. The dependent parameter of the model is the feeling. The values of all parameters within the feeling model are summarized in Table 7. Therefore, the results from the experiment can indicate relations among all parameters, and the relation diagram is illustrated in Figure 5.

According to the relation diagram in Figure 5, there are three line types: line is the direct relation that affects the feelings, dashed line is a moderate relation that influences the emotions, and dotted line can affect the feelings. Thus, there are correlations between PSD of Alpha and Gamma with feeling states. The PSD of Beta needs to apply with the PSD of Gamma, which affects the change of feeling statuses. However, some hidden correlations may affect the alteration of feeling states, such as gender, age, gender with PSD of Alpha, Beta, and Gamma, and age with PSD of Alpha, Beta, and Gamma. Hence, it can be concluded that every independent parameter is related to feeling.

Table 7. Values of the variable in this research

Variables	Values	Type of variables
Gender	Male, Female	Independent
Age	30-39, 40-49, 50-59, greater than 60	Independent
PSD of Alpha	-2.00, 2.00	Independent
PSD of Beta	-2.00, 2.00	Independent
PSD of Gamma	-2.00, 2.00	Independent
Feeling States	Neutral, Anxiety	Dependent

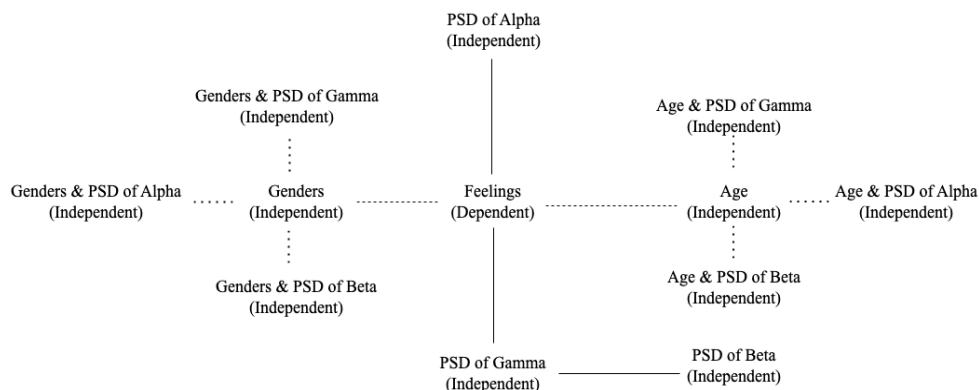


Figure 5. Relation diagram of all parameters

3.2. Model creation

Based on the relation diagram of all parameters, they were compiled with the RapidMiner Studio version 10.3, which is a data analysis tool. The parameters were implemented by the RF algorithm for model generation as a FCM. Moreover, the relationship among the parameters in model creation is many-to-one, as displayed in (1).

$$Feeling = gender + age + (PSD(Alpha, Beta, Gamma)) \quad (1)$$

In (1) is the FCM of changing from gender, age, and the PSD of Alpha, Beta, and Gamma. This model can classify feelings between neural state and anxiety state. However, the model has improved the accuracy with the principal component analysis (PCA). This technique refers to the dimension reduction of data and finding the key components for identifying patterns and relationships hidden within the data. Thus, the FCM has improved the performance of the RF algorithm and reduced the overfitting of the data after analysis with the PCA. Since there are 40 minutes of training data sets, the training data attributes are pc_1, which consists of gender, age, and the PSD of Alpha, Beta, and Gamma. Figure 6 illustrates a tree from RF model.

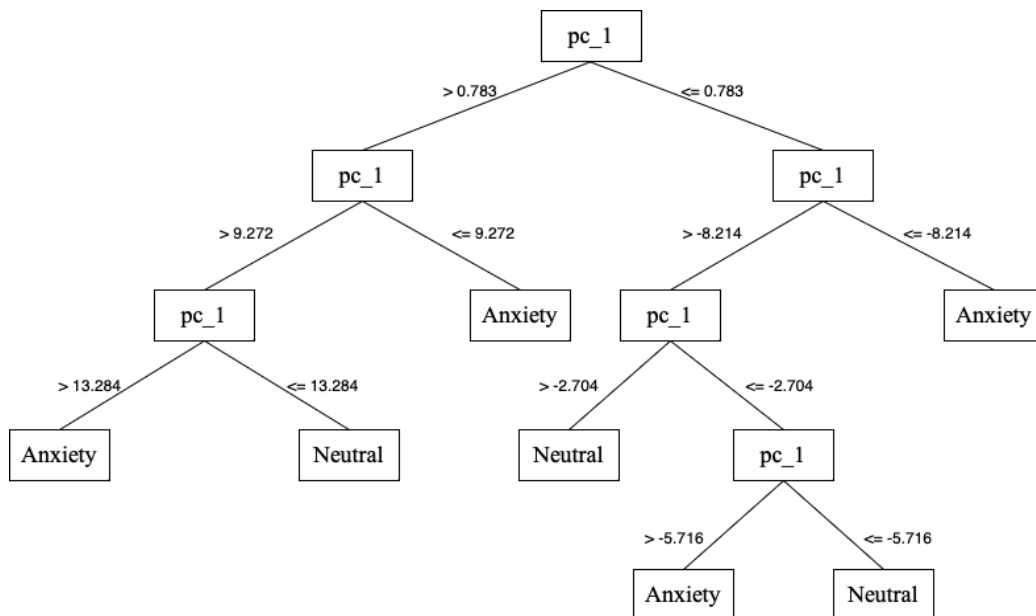


Figure 6. RF algorithm of FCM

3.3. Results

The testing of the data set contains 4 records or 16 minutes. This data is brought to input the FCM for testing accuracy, following the algorithm in Figure 6. The accuracy of the proposed model is computed using true positive (TP), true negative (TN), false positive (FP), and false negative (FN). Precision and recall are then derived from these outcomes, as shown in (2), (3), and (4).

$$Accuracy = (TP + TN) / (TP + TN + FP + FN) \quad (2)$$

$$Precision = TP / (TP + FP) \quad (3)$$

$$Recall = TP / (TP + FN) \quad (4)$$

From the testing result, the precision value is 100%, the recall value is 100%. These values mean that the model can predict the right answer is 1 from the TAPI is 10, the FP is 0, the TN is 0, and the FN is 4. Finally, the accuracy of the FCM is 100%, which means that there is high performance in predicting the feeling.

3.4. Discussion

This research aimed to create a FCM for recognizing anxiety versus normal conditions during blood drawing, based on spectral power features extracted from EEG data. The experimental results showed that the PSD of alpha, beta, and gamma waves exhibited distinguishable patterns that can be leveraged for classification.

Previous research has also investigated EEG-based emotion recognition in medical settings. For instance, Montoya-Martinez *et al.* [13] examined the impact of EEG sensor placement on signal quality and found that specific forehead positions (AF7, AF8) were reliable for capturing emotional states. This finding aligns with our study, where PSD features from the same locations contributed significantly to emotion classification.

Similarly, studies by Choong *et al.* [12] and Cannard *et al.* [14] revealed that variations in EEG spectral components could be associated with stress and anxiety levels. Our results reinforce these findings, particularly with the observed increase in beta and gamma wave activity during anxiety states. However, unlike these studies, which primarily focused on stress detection in general environments, our study applied the methodology specifically to a controlled blood draw scenario, making it more relevant to medical applications.

One key point to address is the reported 100% accuracy of the model. While high accuracy is desirable, such a result raises concerns about potential overfitting due to a limited dataset. Aloy *et al.* [27] highlighted the risk of model overfitting when training with small EEG datasets, suggesting that cross-validation techniques or larger sample sizes are necessary for reliable generalization. To mitigate this risk, future work should expand the dataset and incorporate external validation to confirm the robustness of the model.

Furthermore, while VR has been explored as a method to reduce patient anxiety during medical procedures [3]-[7], its role in this study remains unclear. The inclusion of VR should either be substantiated with empirical data or omitted to maintain a clear research focus.

In summary, this study enhances current knowledge regarding EEG-based anxiety detection and confirms the practicality of employing PSD features with a RF algorithm for real-time emotion recognition. However, future improvements, including dataset expansion and additional validation techniques, are necessary to enhance model reliability.

4. CONCLUSION

The study explored the feasibility of using EEG-based PSD features to classify anxiety and normal states during a blood draw procedure. By analyzing EEG signals from selected electrode positions (AF7, AF8, TP9, TP10) and applying a RF classification model, the study demonstrated that specific frequency bands, particularly alpha, beta, and gamma waves, exhibit distinguishable patterns associated with anxiety.

The results indicate that the proposed FCM is effective in detecting emotional states based on EEG data. However, despite achieving high classification accuracy, a limited sample size and potential overfitting have been identified as key limitations of this study. Further investigations are recommended to increase the dataset size, perform validation with independent participant groups, and incorporate cross-validation techniques for improved generalizability.

In conclusion, the findings of this research enhance the field of EEG-based affective computing through the application of machine learning techniques for real-time anxiety classification. The insights gained from this study could aid in developing non-invasive, AI-driven monitoring systems for medical applications, improving patient safety and personalized care. Future enhancement, including real-time deployment and integration with biofeedback mechanisms, could further optimize the system for clinical use.

FUNDING INFORMATION

Financial support for this research was provided by the Research Institute of Rangsit University, Thailand (Grant Number: 67/2563).

AUTHOR CONTRIBUTIONS STATEMENT

This journal uses the Contributor Roles Taxonomy (CRediT) to recognize individual author contributions, reduce authorship disputes, and facilitate collaboration.

Name of Author	C	M	So	Va	Fo	I	R	D	O	E	Vi	Su	P	Fu
Rawinan Praditsangthong	✓	✓		✓	✓	✓		✓	✓	✓			✓	✓
Ekapong Nopawong		✓	✓			✓	✓	✓	✓	✓	✓	✓		

C : Conceptualization

M : Methodology

So : Software

Va : Validation

Fo : Formal analysis

I : Investigation

R : Resources

D : Data Curation

O : Writing - Original Draft

E : Writing - Review & Editing

Vi : Visualization

Su : Supervision

P : Project administration

Fu : Funding acquisition

CONFLICT OF INTEREST STATEMENT

Authors state no conflict of interest.

INFORMED CONSENT

We have obtained informed consent from all individuals included in this study.

ETHICAL APPROVAL

The was reviewed and approved by the Rangsit University Ethics Review Board (COA.No.RSUERB2021-025). All research procedures involving human participants complied with relevant national regulations, institutional policies, and the ethical standards set forth in the Declaration of Helsinki.

DATA AVAILABILITY

- The data that support the findings of this study are available on request from the corresponding author, E.N. (Ekapong Nopawong). The data, which contain information that could compromise the privacy of research participants, are not publicly available due to certain restrictions.




REFERENCES

- [1] Z. Aulherman, G. Amirulloh, A. Purnomo, G. B. Aji, and S. Supriansyah, "Development of android-based millealab virtual reality media in natural science learning," *Indonesian Journal of Science Education*, vol. 9, no. 1, pp. 1-10, 2021, doi: 10.24815/jpsi.v9i1.18218.
- [2] B. Peixoto, R. Pinto, M. Melo, L. Cabral, and M. Bessa, "Immersive virtual reality for foreign language education: a PRISMA systematic review," *IEEE Access*, vol. 9, pp. 48952–48962, 2021, doi: 10.1109/ACCESS.2021.3068858.
- [3] F. Niix *et al.*, "Virtual reality for pain and anxiety management in children undergoing venipuncture procedures: a systematic review and meta-analysis," *Global Pediatrics*, vol. 4, 2023, doi: 10.1016/j.gped.2023.100060.
- [4] A. Althumairi, M. Sahwan, S. Alsaleh, Z. Alabduljobar, and D. Aljabri, "Virtual reality: is it helping children cope with fear and pain during vaccination," *J. of Multidisciplinary Healthcare*, vol. 14, pp. 2625–2623, 2021, doi: 10.2147/JMDH.S327349.
- [5] R. Nordgard, and T. Lag, "The effects of virtual reality on procedural pain and anxiety in pediatrics: a systematic review and meta-analysis," *Frontiers in Virtual Reality*, vol. 2, 2021, doi: 10.3389/frvir.2021.699383.
- [6] A. Kilic *et al.*, "Using virtual technology for fear of medical procedures: a systematic review of the effectiveness of virtual reality based interventions," *Annals of Behavioral Medicine*, vol. 55, no. 11, 2021, doi: 10.1093/abm/kaab016.
- [7] Q. Huang, J. Lin, R. Han, C. Peng, and A. Huang, "Using virtual reality exposure therapy in pain management: a systematic review and meta-analysis of randomized controlled trials," *Value in Health*, vol. 25, no. 2, pp. 288–301, 2022, doi: 10.1016/j.jval.2021.04.1285.
- [8] O. Czech, A. Wzreciono, A. Rutkowska, A. Guzik, P. Kiper, and S. Rutkowski, "Virtual reality interventions for needle-related procedural pain, fear and anxiety - a systematic review and meta-analysis," *Journal of Clinical Medicine*, vol. 10, no. 15, 2021, doi: 10.3390/jcm10153248.
- [9] J. R. Piazza, S. Merkel, B. Rothberg, J. Gargaro, and K. Kullgren, "Understanding both sides of the blood draw: the experience of the pediatric patient and the phlebotomist," *Patient Experience Journal*, vol. 9, no. 1, pp. 35-45, 2022, doi: 10.35680/2372-0247.1601.
- [10] G. Ozalp, G. Gerceker, D. Ayar, E. Z. Ozdemir, and M. Bektas, "Effects of virtual reality on pain, fear and anxiety during blood draw in children aged 5-12 years old: a randomized controlled study," *Journal of Clinical Nursing*, vol. 29, no. 7-8, pp. 1151-1161, 2020, doi: 10.1111/jocn.15173.
- [11] J. I. Gold, M. Soohoo, A. M. Laikin, A. S. Lane, and M. J. Klein, "Effect of an immersive virtual reality intervention on pain and anxiety associated with peripheral intravenous catheter placement in the pediatric setting: a randomized clinical trial," *JAMA network open*, vol. 4, no. 8, 2021, doi: 10.1001/jamanetworkopen.2021.22569.
- [12] W. Y. Choong *et al.*, "Correlation analysis of emotional EEG in alpha, beta and gamma frequency bands," *Journal of Physics: Conference Series*, vol. 1997, no. 1, 2021, doi: 10.1088/1997/1/012029.
- [13] J. Montoya-Martinez, J. Vanthornhout, A. Bertrand, and A. Francart, "Effect of number and placement of EEG electrodes on measurement of neural tracking of speech," *Plos one*, vol. 16, no. 2, 2021, doi: 10.1371/journal.pone.0246769.
- [14] C. Cannard, H. Wahbehm, and A. Delorme, "Validating the wearable MUSE headset for EEG spectral analysis and Frontal Alpha Asymmetry," *In 2021 IEEE International Conference on Bioinformatics and Biomedicine (BIBM)*, pp. 3603–3610, 2021, doi: 10.1109/BIBM52615.2021.9669778.




- [15] K. S. N. Chan, C. Srisurangkul, N. Depaiwa, and S. Pangkreung, "Detection of driver drowsiness from eeg signals using wearable brain sensing headband," *Journal of Research and Applications in Mechanical Engineering*, vol. 9, no. 2, 2021, doi: 10.14456/jrame.2021.14.
- [16] A. Garg, and V. Mago, "Role of machine learning in medical research: a survey," *Computer science review.*, vol. 40, 2021, doi: 10.1016/j.cosrev.2021.100370.
- [17] Y. Xujing, W. Xinyue, W. Shui-Hua, and Z. Yu-Dong, "A comprehensive survey on convolutional neural network in medical image analysis," *Multimedia Tools and Applications*, vol. 81, pp. 41361–41405, 2021, doi: 10.1007/s11042-020-09634-7.
- [18] R. O. Ogundokun, S. Misra, M. Douglas, R. Damasevicius, and R. Maskeliunas "Medical internet-of-things based breast cancer diagnosis using hyperparameter-optimized neural networks," *Future Internet*, vol. 14, no. 5, pp. 153, 2022, doi: 10.3390/fi14050153.
- [19] C. Sridhar, P. K. Pareek, R. Kalidoss, S. S. Jamal, P. K. Shukla, and S. J. Nuagah, "Optimal medical image size reduction model creation using recurrent neural network and GenPSOWVQ," *Journal of Healthcare Engineering*, 2022, doi: 10.1155/2022/2354866.
- [20] Z. Han, M. Jian, and G. G. Wang, "ConvUNeXt: An efficient convolution neural network for medical image segmentation," *Knowledge-Based Systems*, vol. 253, 2022, doi: 10.1016/j.knosys.2022.109512.
- [21] A. K. Faieq and M. M. Mijwil, "Prediction of of heart diseases utilising support vector machine and artificial neural network," *Indonesian Journal of Electrical Engineering and Computer Science (IJECS)*, vol. 26, no. 1, p. 374, Apr. 2022, doi: 10.11591/ijeecs.v26.i1.pp374-380.
- [22] A. S. Elkorany, M. Marey, K. M. Almustafa, and Z. F. Elsharkawy, "Breast cancer diagnosis using support vector machines optimized by whale optimization and dragonfly algorithms," *IEEE Access*, vol. 10, pp. 69688–69699, 2022, doi: 10.1109/ACCESS.2022.3186021.
- [23] Q. Chen *et al.*, "Regional amplitude abnormalities in the major depressive disorder: a resting-state fMRI study and support vector machine analysis," *Journal of Affective Disorders*, vol. 308, pp. 1–9, 2022, doi: 10.1016/j.jad.2022.03.079.
- [24] A. Alqudah and A. M. Alqudah, "Sliding window based support vector machine system for classification of breast cancer using histopathological microscopic images," *IETE Journal of Research*, vol. 68, no. 1, pp. 59–67, 2022, doi: 10.1080/03772063.2019.1583610.
- [25] H. Kutrani and S. Eltalhi, "Decision tree algorithms for predictive modeling in breast cancer treatment," *2022 IEEE 2nd International Maghreb Meeting of the Conference on Sciences and Techniques of Automatic Control and Computer Engineering (MI-STA)*, pp. 223–227, 2022, doi: 10.1109/MI-STA54861.9837762.
- [26] P. Dinesh and P. Kalyanasundaram, "Medical image prediction for diagnosis of breast cancer disease comparing the machine learning algorithms: SVM, KNN, logistic regression, random forest, and decision tree to measure accuracy," *ECS Transactions*, vol. 107, 2022, doi: 10.1063/5.0203746.
- [27] A. Aloy, M. G. Anluja, M. P. Kishore, S. Chitti, R. B. Vallabhaneni, and N. Renuka, "EEG signal classification automation using novel modified random forest approach," *Journal of Scientific & Industrial Research*, vol. 82, no. 1, pp. 101-108, 2023, doi: 10.56042/jsir.v82i1.70213.
- [28] R. Haba, G. Singer, S. Naftali, M. R. Kramer, and A. Ratnovsky, "A remote and personalised novel approach for monitoring asthma severity levels from EEG signals utilizing classification algorithms," *Expert Systems with Applications*, vol. 223, 2023, doi: 10.1016/j.eswa.2023.119799.

BIOGRAPHIES OF AUTHORS



Rawinan Praditsangthong    is lecturer at college of Digital Innovation Technology, Rangsit University, Thailand. She received the B.Sc. degree in Computer Science and the M.Sc. degree in Information Technology from the Rangsit University, Thailand. She received the Ph.D. degree in Computer Science and Information Technology, Department of Mathematics and Computer Science, the Chulalongkorn University, Thailand. Her research areas are machine learning, facial recognition, artificial intelligence, chatbot, healthcare emotion recognition, web and mobile development, computer vision, image processing and fintech. Her research interests include reinforcement learning and AI bot (text or voice). She can be contacted at email: rawinan.p@rsu.ac.th.



Ekapong Nopawong    received the Bachelor of Engineering degree in Computer Engineering from the Suranaree University of Technology, Thailand, and the Master of Arts degree in Multimedia Technology from the Swinburne University of Technology, Australia. He is currently a Lecturer at Department of Computer Game and Esports, College of Digital Innovation Technology, Rangsit University, Thailand. His research interests include game design, game development augmented reality (AR), virtual reality (VR), mixed reality (MR), serious game, computer vision, simulation, and AI. He can be contracted at email: ekapong.n@rsu.ac.th.